Appl. Phys. B 68, 495–499 (1999)

Applied Physics B
Lasers
and Optics
© Springer-Verlag 1999

Invited paper

Femtosecond electron and spin dynamics probed by nonlinear optics

G.P. Zhang, W. Hübner

Max-Planck-Institut für Mikrostrukturphysik, Weinberg 2, D-06120 Halle, Germany
(Fax: +49-345/5511-223, E-mail: zhang@mpi-halle.mpg.de)

Received: 20 September 1998

Abstract. A theoretical calculation is performed for the ultrafast spin dynamics in nickel using an exact diagonalization method. The present theory mainly focuses on the situation where the intrinsic charge and spin dynamics is probed by the nonlinear (magneto-)optical responses on the femtosecond time scale, i.e. optical second harmonic generation (SHG) and the nonlinear magneto-optical Kerr effect (NOLIMOKE). It is found that the ultrafast charge and spin dynamics are observable on the time scale of 10 fs. The charge dynamics proceeds ahead of the spin dynamics, which indicates the existence of a spin memory time. The fast decay results from the loss of coherence in the initial excited state. Both the material specific and experimental parameters affect the dynamics. We find that the increase of exchange interaction accelerates mainly the spin dynamics rather than the charge dynamics. A reduction of the hopping integrals, such as present at interfaces, slows down the spin dynamics significantly. Furthermore, it is found that a spectrally broad excitation yields the intrinsic speed limit of the charge (SHG) and spin dynamics (NOLIMOKE) while a narrower width prolongs the dynamics. This magnetic interface dynamics should then become accessible to state-of-the-art time-resolved nonlinear-optical experiments.

PACS: 78.47.+p; 78.20.Ls; 75.70.-i

Recently ultrafast spin dynamics in ferromagnetic metals has attracted a great deal of attention due to its possible applications, for example, in ultrafast magnetic gates. The experimental observation was that, upon the excitation of a femtosecond laser pulse, a sharp decrease of the magnetization occurs on a time scale of 100 fs [1–4], which is far beyond the characteristic time scale of spin–lattice interaction. Similar results have been independently found in pump and probe linear magneto-optics, nonlinear magneto-optics and two-photon photoemission. However the interpretation of this behavior has not been given on the same footing and remains somewhat speculative. Reconciliation of these intriguing results from different experimental processes such as linear and nonlinear optics is a crucial matter and is one of the goals of the present theoretical study. Moreover, the demagnetization is very similar to the conventional one [2].

In the SHG experiment [2], the $M(T)$ curve is established after the electron thermalization is finished while the electron and lattice have not reached a common equilibrium yet, which indicates a purely electronic feature of the ultrafast spin dynamics. Traditionally the spin–lattice coupling sets the speed limit of the demagnetization process, typically about 100 ps [5], but here this is evidently not the case. Our previous theoretical studies clearly demonstrated that the dephasing of initial states is the origin of the spin dynamics on the femtosecond time scale [6, 7], as probed by transient reflectivities and linear magneto-optics. We found that the intrinsic speed limit is about 10 fs. This mechanism is a pure quantum effect, resulting from the interplay between band structure and electron correlation. In this paper, we focus on the *nonlinear* optical response of spin dynamics. We take a Ni monolayer as an example.

This paper is arranged as follows. In Sect. 1, we discuss our theoretical scheme while the main results are given in Sect. 2. Finally, the conclusions are presented in Sect. 3

1 Theoretical scheme

It is well-established that in ferromagnetic transition metals, in particular in Ni, the electron correlation plays an important role even in the ground state and possesses a significant impact on the excited states, as evidenced e.g. by the famous photoemission satellite structure [8]. This becomes especially true in the nonlinear optical process on the ultrafast time scale where highly excited states are frequently involved. Therefore, we employ an exact-diagonalization method which explicitly avoids a perturbative treatment of electron correlation. Within our scheme, one does not need to introduce any damping term to obtain a correct dephasing time. Our previous

results showed that the typical time scale is basically set by the dispersion of the bands and the strength of electron correlation. We begin with a generic Hamiltonian

$$H = \sum_{i,j,k,l,\sigma,\sigma',\sigma'',\sigma'''} U_{i\sigma,j\sigma',l\sigma''',k\sigma''} c^{\dagger}_{i\sigma} c^{\dagger}_{j\sigma'} c_{k\sigma''} c_{l\sigma'''} + \sum_{\nu,\sigma,K} \mathcal{E}_{\nu}(K) n_{\nu\sigma}(K) + H_{\mathrm{SO}} \quad (1)$$

where $U_{i\sigma,j\sigma',l\sigma''',k\sigma''}$ is the on-site electron interaction, which can be described in full generality by three parameters: the Coulomb repulsion U, the exchange interaction J, and the exchange anisotropy ΔJ [9]. The set of parameters used for Ni is given in [10]. $c^{\dagger}_{i\sigma}$ ($c_{i\sigma}$) are the usual creation (annihilation) operators in the orbital i with spin σ ($\sigma = \uparrow, \downarrow$). $\mathcal{E}_{\nu}(K)$ is the single-particle energy spectrum for band ν of the nickel monolayer. $n_{\nu\sigma}(K)$ is the particle number operator in momentum space. H_{SO} is the spin–orbit coupling. Since this is a typical many-body problem, one cannot solve it without simplification. In order to obtain a tractable model, we first build a two-hole basis set. Within this basis set, for each Ni atom, the dimension of the Hilbert space is 66. The matrix elements of electron correlation for each atom can be obtained analytically. For each K point, the electron correlation is embedded in the crystal field as given by the band structure. This treatment of correlations is analogous to a frequency-dependent self-energy correction. Within this simplification, we are able to exactly diagonalize the Hamiltonian for each K point explicitly.

In order to characterize the spin and charge dynamics clearly, we calculate both these intrinsic quantities: $S_z(t) = \langle\Psi(0)|\hat{S}_z|\Psi(t)\rangle$ and $N(t) = \langle\Psi(0)|\hat{N}|\Psi(t)\rangle$, and the nonlinear (magneto-)optical susceptibilities $\chi^{(2)}_{xzz}$ and $\chi^{(2)}_{zzz}$. Here $\hat{S}_z = \frac{1}{2}(\hat{n}_{\uparrow} - n_{\downarrow})$, $\hat{N} = (\hat{n}_{\uparrow} + n_{\downarrow})$, which are directly related to the observable NOLIMOKE and SHG yields, respectively. Since $\left|\chi^{(2)}_{xzz}(\omega, t)\right|$ and $\left|\hat{S}_z(t)\right|$ mainly reflect the spin response while $\left|\chi^{(2)}_{zzz}(\omega, t)\right|$ and $\left|\hat{N}(t)\right|$ reflect the charge response, they will be used as indicators to evaluate spin and charge evolutions, respectively. We find:

$$\chi^{(2)}_{xzz}(\omega, t) = \sum_{k,l,l',l''} \left(\frac{p(E_{kl''}, t) - p(E_{kl'}, t)}{E_{kl''} - E_{kl'} - \omega + \mathrm{i}\eta} - \frac{p(E_{kl'}, t) - p(E_{kl}, t)}{E_{kl'} - E_{kl} - \omega + \mathrm{i}\eta} \right) \Big/ (E_{kl''} - E_{kl} - 2\omega + \mathrm{i}2\eta) \times \left(\langle kl|\hat{S}_z|kl\rangle + \langle kl'|\hat{S}_z|kl'\rangle + \langle kl''|\hat{S}_z|kl''\rangle - 3/2 \right) \quad (2)$$

$$\chi^{(2)}_{zzz}(\omega, t) = \sum_{k,l,l',l''} \left(\frac{p(E_{kl''}, t) - p(E'_{kl}, t)}{E_{kl''} - E_{kl'} - \omega + \mathrm{i}\eta} - \frac{p(E_{kl'}, t) - p(E_{kl}, t)}{E_{kl'} - E_{kl} - \omega + \mathrm{i}\eta} \right) \Big/ (E_{kl''} - E_{kl} - 2\omega + \mathrm{i}2\eta) \quad (3)$$

where $|kl\rangle$ is the eigenstate with the eigenvalue E_{kl}; $p(E_{kl}, t) = \langle\Psi(t)|kl\rangle$.

2 Results

Before we come to our main results, we would like to demonstrate that our Hamiltonian can reasonably describe some basic experimental results. It has been well-established that a prerequisite for acquiring a ferromagnetic ground state is a nonzero Coulomb interaction U and exchange interaction J. We can simply check this by setting both U and J to zero. Doing so, we find that the ground state is a singlet, i.e. paramagnetic state, which contradicts the ferromagnetic nature of nickel. This proves the importance of U and J. Once we use the generic sets of U and J of nickel, we obtain a triplet as its ground state, from which we can calculate the magnetic moment, $0.88\mu_{\mathrm{B}}$. This magnetic moment is larger than that in the bulk material, which is consistent with the experimental observation. In this case, the satellite structure well-known from photoemission experiments also appears quite naturally in the spectrum.

In Fig. 1, we firstly show the effect of exchange coupling J on the $|\chi^{(2)}_{xzz}(\omega, t)|$ and $|\chi^{(2)}_{zzz}(\omega, t)|$ as a function of time t. The probe frequency ω is fixed at 2 eV. The initial state is prepared to be 2 eV above the ground state with a Gaussian broadening as large as 20 eV, which opens almost all the possible decay channels. Such a large distribution width cor-

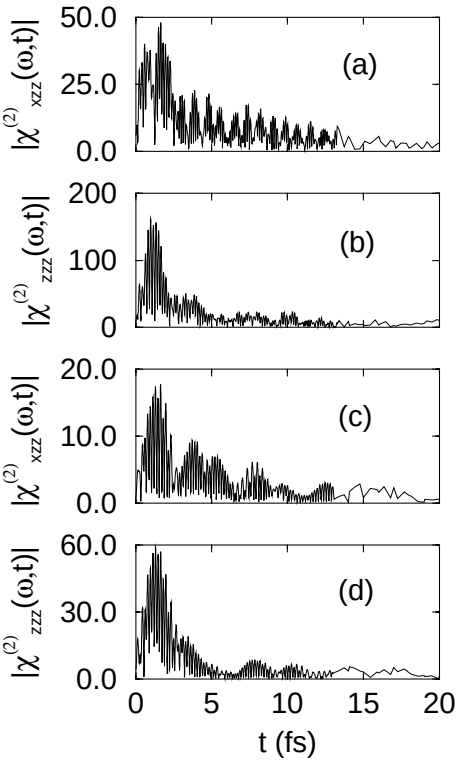

Fig. 1a–d. The femtosecond time evolution of the nonlinear magneto-optical and optical responses, $\left|\chi^{(2)}_{xzz}(\omega, t)\right|$ and $\left|\chi^{(2)}_{zzz}(\omega, t)\right|$, respectively. Here the initial excited state is prepared 2 eV above the ground state with a Gaussian broadening as wide as 20 eV. In **a** and **b**, a set of generic parameters of nickel is used; in **c** and **d**, the exchange interaction J is reduced to $J_0/10$ while the rest of the parameters are kept unchanged. The spin dynamics is delayed with respect to charge dynamics, which indicates the existence of a spin memory effect. Additional 'bunching' occurs, which has not been found for the linear pump-probe responses of Ni. $\left|\chi^{(2)}_{xzz}(\omega, t)\right|$ oscillates with a larger period

responds to a very large laser spectral width. As previously explained, this choice aims at revealing the real *intrinsic* speed limit of the spin dynamics in our system, which is then not delayed by experimental constraints. In Figs. 1a and 1b, the generic parameters of Ni monolayers are used. There are several interesting features that should be mentioned. One notices in Fig. 1a that $|\chi^{(2)}_{xzz}(\omega, t)|$ first rises very quickly and reaches its maximum at about 2–3 fs. Then $|\chi^{(2)}_{xzz}(\omega, t)|$ has a sharply decreasing envelope and oscillates with a very short period. The dynamics of $|\chi^{(2)}_{xzz}(\omega, t)|$ settles down around 10 fs (decay to $1/e$ of maximum), which indicates the complete dephasing. As already mentioned, $|\chi^{(2)}_{xzz}(\omega, t)|$ signifies the spin relaxation process. Thus we estimate that the spin relaxation time is about 10 fs, which is consistent with our previous results for time-resolved linear (magneto-)optics based on $|\chi^{(1)}_{xy}|$ and $|\chi^{(1)}_{zz}|$. For the charge dynamics, we see a different scenario. In Fig. 1b, $|\chi^{(2)}_{zzz}(\omega, t)|$ is plotted as a function of time t. One sees that $|\chi^{(2)}_{xzz}(\omega, t)|$ requires nearly the same time to reach its maximum as $|\chi^{(2)}_{xzz}(\omega, t)|$ does, but that the subsequent decay occurs more sharply and strongly. Around 5 fs, the value of $|\chi^{(2)}_{zzz}(\omega, t)|$ is already close to the equilibrium data. This means that the dephasing already becomes strong for the charge dynamics before it does for the spin dynamics. If one compares Figs. 1a with 1b, one sees a clear difference between spin and charge dynamics. Basically the spin dynamics lasts about twice as long as the charge dynamics. This has an important consequence as it demonstrates the spin memory effect: though the charge dynamics finishes, the spin dynamics is still alive, which is crucial for future applications. The main difference between the time-resolved nonlinear response and the linear one, which is particularly evident for the magnetic dynamics, consists in an additional 'bunching' of the structures resulting from the simultaneous presence of ω and 2ω resonances in (2) and (3).

In order to get a handle on the microscopic origin of the observed magnetic dynamics, we try to investigate the effect of the on-site exchange coupling J. We reduce J to $J_0/10$. The corresponding time-dependences of $|\chi^{(2)}_{xzz}(\omega, t)|$ and $|\chi^{(2)}_{zzz}(\omega, t)|$ are shown in Figs. 1c and 1d, respectively. It can be seen that $|\chi^{(2)}_{xzz}(\omega, t)|$ first rises within 2 fs. After that a recurrence appears with a rather large amplitude. Compared with Fig. 1a, $|\chi^{(2)}_{xzz}(\omega, t)|$ oscillates with a longer 'bunching' period and the loss of coherence is weaker. We estimate that the relaxation time is about 10 fs but the period is nearly twice as long as that in Fig. 1a. This demonstrates that the decrease of exchange interaction prolongs the period of oscillations. For the charge dynamics, the change going from J_0 to $J_0/10$ is relatively small. This can be seen from Fig. 1d where we plot $|\chi^{(2)}_{zzz}(\omega, t)|$ as a function of time t. Comparing Figs. 1b and 1d, one finds that the overall variation of $|\chi^{(2)}_{zzz}(\omega, t)|$ with time is nearly identical. This is understandable since the exchange interaction acts more directly on the spin degree of freedom by changing the spin dependence of the electronic many-body states microscopically. Consequently, the spin dynamics will be affected more strongly than the charge dynamics. However electrons even with different spin-orientations play a similar role for the charge dynamics. Thus, the charge dynamics is basically independent of the spin state. That is why the exchange interaction does not affect the charge dynamics significantly.

Next, we wish to gain some physical insights into the effects of the experimental constraints, such as the spectral width of the excited state distribution, on the spin dynamics. In Fig. 2, we perform a detailed comparison between those experimental observables and intrinsic quantities (i.e., $|\hat{S}_z(t)|$, $|\hat{N}_z(t)|$). The initial excited state is prepared 2 eV above the ground state with a Gaussian broadening of now only 0.2 eV, which simulates a narrow laser spectral width, in contrast to the previously used width of 20 eV. This allows us to see the effect of the laser spectral width clearly. All the parameters for the Hamiltonian are the generic set of parameters of Ni. In Figs. 2a and 2b, we show the results up to 40 fs. The abscissa and ordinate in Figs. 2a and 2b denote the real and imaginary parts of the intrinsic spin and charge dynamics, $S_z(t)$ and $N(t)$, respectively. Note that these quantities cannot directly be observed and are only theoretically accessible. The arrows refer to the time direction and the centers are the final positions of $S_z(t)$ and $N(t)$. One notices that the spin dynamics needs about six cycles to reach its final value while for the charge dynamics only three cycles are needed. This demonstrates again that the spin dynamics is delayed with respect to the charge dynamics. We find that comparing those intrinsic quantities one can see a clear difference between spin and charge responses, which is not blurred by the details of the experimental conditions. Nevertheless, from our results, one can still identify the differences also in the nonlinear optical and magneto-optical responses. We show the results in Figs. 2c and 2d. In Fig. 2c, $|\chi^{(2)}_{xzz}(\omega, t)|$ is plotted as a function of time up to 80 fs. One may notice that a decay occurs within 30–40 fs, which is consistent with our previous linear results obtained from $|\chi^{(1)}_{xy}|$ and $|\chi^{(1)}_{zz}|$ [6]. SHG probes more bands, which causes more 'beating' and 'bunching'. This might then

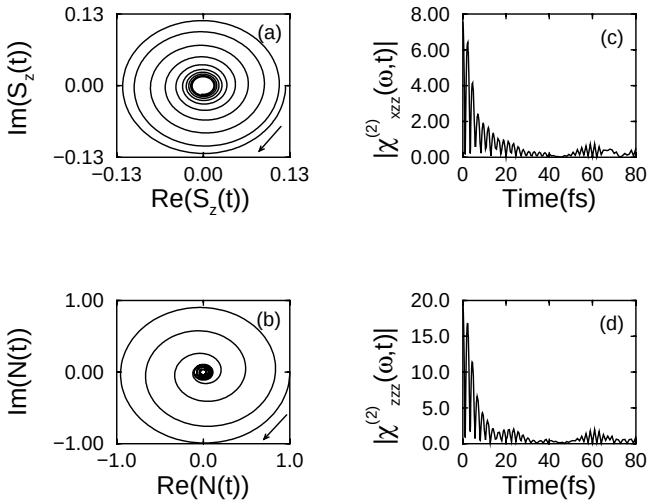

Fig. 2a–d. Femtosecond time evolution of the intrinsic spin (**a**) and charge (**b**) dynamics, which is not directly observable, in comparison with the magneto-optical (**c**) and optical (**d**) response functions. $\left|\hat{S}_z(t)\right|$ and $\left|\hat{N}(t)\right|$, **a** and **b** show the clearly different behavior between spin and charge dynamics. Here the initial state is also prepared to be 2 eV above the ground state, but the spectral width is 0.2 eV. The other parameters are taken as the generic parameters of Ni. The time interval is [0,40 fs] for (**a**) and (**b**). The calculated intrinsic (**a**, **b**) and experimentally accessible (**c**, **d**) quantities show a strong dependence on the laser spectral width (corresponding to the initial excited state width). Comparing with Fig. 1, we notice that for the same set of generic parameters, the decrease of the laser spectral width yields a slower decay of the spin and charge response

result in an effectively slower response than that seen in linear pump–probe experiments, in addition to the slowing down which results from the narrower bandwidth at interfaces. For $|\chi^{(2)}_{zzz}(\omega, t)|$ we present the results in Fig. 2d. Comparing with $|\chi^{(2)}_{xzz}(\omega, t)|$ in Fig. 2c, $|\chi^{(2)}_{zzz}(\omega, t)|$ drops even more sharply. One can see a clear drop at 18 fs, which sets its relaxation time for charge dynamics. A delay of about 10 fs between spin and charge responses is found for this specific set of parameters. Comparing Figs. 1a and 2c, one can immediately see that a narrow initial state distribution width prolongs the relaxation process. In Fig. 1, one knows that the relaxation process basically finishes within 10 fs, but here the relaxation time is around 30–40 fs.

Finally, as our previous studies have already shown [6, 7] for the linear pump-probe calculations, the band structure will also influence the relaxation process. Its effect is actually very significant. Our results on $|\chi^{(1)}_{xy}|$ and $|\chi^{(1)}_{zz}|$ already showed that the hopping integrals can modify the relaxation process strongly. Analogously, this will be reflected in the nonlinear optical responses $|\chi^{(2)}_{xzz}(\omega, t)|$ and $|\chi^{(2)}_{zzz}(\omega, t)|$. In order to investigate the effect of the band structure, we reduce the hopping integrals to one-tenth of the original nickel hopping integrals while keeping the rest of parameters unchanged. Here, the initial excited state is also prepared 2 eV above the ground state with a Gaussian broadening of 20 eV. The results are shown in Fig. 3. One finds that the change of both $|\chi^{(2)}_{xzz}(\omega, t)|$ and $|\chi^{(2)}_{zzz}(\omega, t)|$ with time is very different from the previous ones. From Fig. 3a, one notices that *xzz* increases sharply within 5 fs. The strong oscillation lasts about 20 fs, where no clear decay can be seen. The outline of $|\chi^{(2)}_{xzz}(\omega, t)|$ ranging from 0 fs to 20 fs forms a broad peak. After 20 fs, dephasing occurs, but the envelope of $|\chi^{(2)}_{xzz}(\omega, t)|$ decays only slowly. Comparing Figs. 1a and 1b with Figs. 3a and 3b, respectively, one sees that the reduction of the hopping integrals slows down both the spin and charge dynamics considerably. The envelope of $|\chi^{(2)}_{xzz}(\omega, t)|$ now decays on the time scale of 30–40 fs. The appreciable fast oscillation in the long-time tail survives beyond 80 fs. Comparing Figs. 3a and 3b with Figs. 2c and 2d, respectively, indicates that the elementary oscillations are more rapid. Thus from the comparison of all the three figures, we conclude that the reduction of the excited states distribution width affects the elementary oscillation more strongly than the envelope of the spin and charge responses while decreasing the hopping integrals does the opposite and mainly slows down the response envelope of $|\chi^{(2)}_{xzz}(\omega, t)|$ and $|\chi^{(2)}_{zzz}(\omega, t)|$. It is remarkable that in all cases the spin memory effect persists. In addition, we would like to point out that the change of band structure imposed by spin–orbit coupling also affects the spin dynamics observed in nonlinear magneto-optical experiments. For linear time-resolved magneto-optical experiments, this has been demonstrated theoretically (see [6, 7]). We found that spin–orbit coupling had to be raised to an unphysically large value of 1 eV (the generic value of spin–orbit coupling in nickel is 0.07 eV) in order to be relevant for the spin dynamics. Thus we do not expect any major influence from spin–orbit coupling on the 10 fs spin dynamics of transition metals in the valence band.

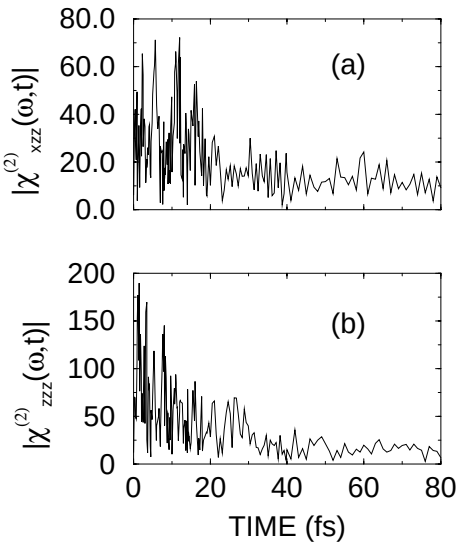

Fig. 3. The femtosecond time evolution of the nonlinear magneto-optical and optical responses, $\left|\chi^{(2)}_{xzz}(\omega, t)\right|$ and $\left|\chi^{(2)}_{zzz}(\omega, t)\right|$, respectively. The same initial condition has been used as in Fig. 1 except for the hopping integrals which are taken to be one-tenth of the original ones. It turns out that the change of band structure has a significant impact on spin and charge dynamics. It slows down the dynamics by modifying the envelopes of the response functions $\left|\chi^{(2)}_{xzz}(\omega, t)\right|$ and $\left|\chi^{(2)}_{zzz}(\omega, t)\right|$

3 Conclusions

In conclusion, we have performed an exact-diagonalization scheme to study the spin dynamics in ferromagnetic nickel on the femtosecond time scale. This study is exclusively devoted to the nonlinear optical responses. We first checked that our Hamiltonian gives a correct ferromagnetic ground state and a correct order of magnitude of the magnetic moment, which is larger than its value in bulk materials, as is physically expected. For a generic set of Ni parameters, the intrinsic speed limit of spin dynamics is about 10 fs, which is on a similar time scale as revealed by $|\chi^{(1)}_{xy}|$ although additional 'bunching' structure appears for the nonlinear time-resolved magneto-optical response. Our theory clearly yields the memory effect of the spin dynamics also in nonlinear optics. It is found that the spin dynamics is delayed with respect to the charge dynamics. The spin dynamics survives even when the charge dynamics ceases. This is very important for future applications, such as ultrafast magnetic gates. We also examined the effect of exchange interaction. It is found that a decrease of the exchange interaction prolongs the relaxation process. In particular, we noticed that for a smaller exchange interaction J the spin response 'bunches' with longer periods. This again confirms our earlier results that the observed spin dynamics results from the spin dependent (J-dependent) dephasing in the excited many-body states. In that sense, SHG and NOLIMOKE reveal the same fundamental physics as time-resolved linear (magneto)-optics. In order to give more insight into the spin dynamics, we also calculated some intrinsic quantities, from which we see a clearer difference between spin and charge dynamics. In addition, we studied the laser width effect on the spin dynamics. It shows that a narrow spectral width clearly slows down the dynamics. This is understandable as, for a smaller spectral width, the number of populated states is smaller. The dissipation becomes weaker and eventually the spin dynamics is

prolonged significantly. Finally we studied the effect of the band structure on the spin dynamics. We found that the reduction of the hopping integrals slows down both the spin and charge dynamics by modifying the envelope of the response functions $|\chi^{(2)}_{xzz}(\omega, t)|$ and $|\chi^{(2)}_{zzz}(\omega, t)|$. This is different from the effect of a narrower distribution width, where one basically prolongs the oscillation periods. It is important to note that materials with a small hopping integral correspond to nanostructure materials, clusters, quantum well states, magnetic insulators (such as oxides), defects, and impurities. Thus it is expected that with the presence of those nanostructure materials, the observed dynamics will be significantly slower. Naturally, this is very significant for the design of materials for ultrafast magnetic devices. Finally and mostly importantly, the processes which we investigated all exhibit the spin memory effect, a crucial property for future applications.

References

1. E. Beaurepaire, J.-C. Merle, A. Daunois, J.Y. Bigot: Phys. Rev. Lett. **76**, 4250 (1996)
2. J. Hohlfeld, E. Matthias, R. Knorren, K.H. Bennemann: Phys. Rev. Lett. **78**, 4861 (1997); *ibid.* **79**, 960 (1997) (erratum)
3. M. Aeschlimann, M. Bauer, S. Pawlik, W. Weber, R. Burgermeister, D. Oberli, H.C. Siegmann: Phys. Rev. Lett. **79**, 5158 (1997)
4. A. Scholl, L. Baumgarten, W. Eberhardt: Phys. Rev. Lett. **79**, 5146 (1997)
5. A. Vaterlaus, T. Beutler, F. Meier: Phys. Rev. Lett. **67**, 3314 (1991)
6. W. Hübner, G.P. Zhang: Phys. Rev. B **58**, R5920 (1998)
7. W. Hübner, G.P. Zhang: J. Magn. Magn. Mater. **189**, 101 (1998)
8. P. Fulde: *Electron Correlation in Molecules and Solids*, 3rd edn. (Springer, Berlin, Heidelberg 1995); J. Wahle, N. Blümer, J. Schling, K. Held, D. Vollhardt: cond-mat/9711242
9. W. Hübner, L.M. Falicov: Phys. Rev. B **47**, 8783 (1993); C. Moore: *Atomic Energy Levels*, Natl. Bur. Stand. (U.S.) (U.S. GPO, Washington DC 1971)
10. W. Hübner: Phys. Rev. B **42**, 11553 (1990)